J. Fluid Mech. (2004), *vol.* 502, *pp.* 41–63.
DOI: 10.1017/S0022112003007250 Printed in the United Kingdom

Coalescing axisymmetric turbulent plumes

By N. B. KAYE[1] AND P. F. LINDEN[2]

[1]Department of Civil and Environmental Engineering, Imperial College of Science, Technology and Medicine, Imperial College Road, London, SW7 2BU, UK

[2]Department of Mechanical and Aerospace Engineering, University of California, San Diego, 9500 Gilman Drive, La Jolla, CA 92093-0411, USA

(Received 27 March 2003 and in revised form 15 August 2003)

The coalescence of two co-flowing axisymmetric turbulent plumes and the resulting single plume flow is modelled and compared to experiments. The point of coalescence is defined as the location at which only a single peak appears in the horizontal buoyancy profile, and a prediction is made for its height. The model takes into account the drawing together of the two plumes due to their respective entrainment fields. Experiments showed that the model tends to overestimate the coalescence height, though this discrepancy may be partly explained by the sensitivity of the prediction to the entrainment coefficient. A model is then developed to describe the resulting single plume and predict its virtual origin. This prediction and subsequent predictions of flow rate above the merge height compare very well with experimental results.

1. Introduction

The coalescence of turbulent plumes to form a single plume is a process that occurs in many situations. Ventilated enclosures with multiple heat sources, such as work spaces with electronic equipment or occupied lecture theatres, contain turbulent plumes that rise above heat sources and interact. Their interaction will affect the resulting ventilation flow (Linden 1999). Turbulent plumes rising from smokestacks in close proximity can also interact. In this case the rise height of the plumes into a stratified atmosphere will depend on the nature of the interaction. Despite these numerous applications, very little work has been done on the question of how two turbulent plumes coalesce to form a single plume. This paper describes a model for the merging of two turbulent plumes, and for the resulting single plume.

1.1. *Interacting laminar plumes*

Pera & Gebhart (1975) studied the interaction of laminar parallel line plumes, merging to form a single plume. They conducted experiments in which the relative strengths of the two plumes and the ratio of the plume source lengths to their separation were varied. They presented a model for this merging process based on the restriction of the entrainment into each plume by the presence of the other. They observed that for plumes of significantly different strengths, the weaker plume was deflected considerably more than the stronger plume. Some experiments were also done with axisymmetric plumes. Although no model was presented for how the axisymmetric plumes coalesce, they observed that the interaction was weaker than for line plumes.

Moses, Zocchi & Libchaber (1993) presented work focused on the starting cap of laminar plumes, but also briefly examined the coalescence height z_m of axisymmetric

laminar plumes. They found that z_m is given by

$$z_m = 0.06\sigma\left(\frac{F}{\nu^3}\right)d_0^2, \tag{1.1}$$

where d_0 is the source separation, ν the kinematic viscosity, σ the Prandtl number, and F is the buoyancy flux defined in Batchelor (1954) and given by

$$F = \frac{\Phi g}{C_p \rho_0 T_0}, \tag{1.2}$$

where Φ is the heat flux of the plume, C_p is the specific heat, ρ_0 is a reference density, g is the gravitational acceleration and T_0 in degrees Kelvin is a reference temperature.

The main difference between merging laminar and turbulent plumes is that turbulent plumes are independent of the fluid viscosity. However, there are two key points of similarity: laminar axisymmetric plume interaction results in the plumes coalescing further from their sources than for the case of line plumes, and the weaker plume tends to be deflected significantly more than the stronger plume. As we discuss below, both of these effects are observed in turbulent plume interaction.

1.2. *Interacting turbulent plumes*

The interaction of turbulent plumes has a wide range of applications, and has been mainly examined in studies related to these applications. Rouse, Baines & Humphreys (1953) studied turbulent line plumes to determine whether they would be effective in removing fog from British airfields during World War II. They presented velocity and temperature measurements, along with dimensionless isotherms and streamlines. The plumes were observed to draw together sharply so that no ambient fluid remained between them. This meant that, even at very low heights, it was not possible to distinguish two separate plumes. All heights scaled on the plume source separation χ_0, and the velocity was found to scale on $(\hat{F}/L)^{1/3}$, where $\hat{F}/L$ is the buoyancy flux per unit length of source. These results indicate that the problem is independent of fluid properties, as expected.

Ching *et al.* (1996) investigated the transient problem of how two equal line plumes are drawn together after starting at the same time, in the context of plumes descending from leads formed in cracked ice sheets. They observed that initially the two plumes descend separately, and are relatively unaffected by each other. However, after reaching a certain height, they are drawn together more strongly, due to the finite volume of fluid between the plumes that cannot be replenished. The time scale for this development is $\chi_0/(\hat{F}/L)^{1/3}$. In steady-state pictures (shown in figure 6(f) of Ching *et al.* 1996) the axes of the plumes meet at a height of approximately χ_0 (also observed by Tritton 1988, p. 186).

The problem of merging axisymmetric turbulent plumes is virtually untouched. Baines (1983) published the first results relating to this problem in a paper, not on merging plumes, but on flow rate measurements in turbulent plumes. Baines plotted the plume flow-rate Q (in the form $(Q^3/\hat{F})^{1/3}$) against the vertical distance from the source z, where F is the buoyancy flux in the plume. The distance from the source at which flow rate measurements were taken varied from $0.25\chi_0$ to $11\chi_0$ and Froude numbers are quoted for the source, allowing virtual origin corrections to be made. Only two experiments were performed, both at the same separation, and with equal plumes. One important observation was that, once the plumes had joined, the volume flow rate Q of the combined plume rapidly approached the five-thirds power law seen in fully developed plumes ($Q \sim F^{1/3}z^{5/3}$). This transition occurred over a height

approximately equal to the plume diameter at the height of merging. However, the adjustment of the combined plume from its newly merged state to being circular in cross section took considerably longer. This implies that the plumes obeyed the scaling law for flow rate predicted by dimensional analysis despite not being self-similar. This rapid transition between two-plume and single-plume flow-rate scaling behaviour is important in modelling these flows, as it allows the problem to be separated into two parts: first, how the plumes coalesce, and then how they behave after coalescence.

Brahimi & Doan-Kim-Son (1985) measured the velocity and temperature profiles of merging axial turbulent plumes using temperature probes and a laser-Doppler anemometer. They presented results for an experiment, performed using thermal plumes created by using heated disks. A development region was observed between the height where the plumes begin to interact and the height where a fully self-similar single plume has developed. However the thermal plumes were not fully developed when they started to interact so the results have only limited application to the general problem of coalescing pure turbulent plumes.

These purely experimental papers were not concerned with the process of coalescence. The first work on the merging process was by Bjorn & Nielsen (1995), who made velocity measurements above two equal turbulent plumes in the plane of symmetry containing the plume sources. They modelled the flow by assuming that the velocities of the plumes could simply be added, an idea first suggested by Davidson, Papps & Wood (1994), who modelled an infinite line of equal plumes as they merged into a line plume. The model does not take into account the drawing together of the two plumes caused by their respective entrainment fields, and again the experimental plumes were not fully developed when they interacted and merged.

The basic problem of how two fully developed axisymmetric turbulent plumes interact with each other while merging remains unsolved, along with the question of how to describe the resulting single plume. Furthermore, no work exists on unequal co-flowing plumes. This paper addresses the problem for two unequal axisymmetric turbulent plumes with sources at the same height. A model for the coalescence is described in § 2 and the properties of the resulting single plume is given in § 3. Experiments on the merging of two plumes are described and compared with the model in § 4. Our conclusions are given in § 5.

2. Plume merging height

Pera & Gebhart (1975) have shown that buoyancy flux, separation, viscosity, and Prandtl number govern the merging of laminar plumes. The fluid properties do not influence the flow of turbulent plumes and, therefore, the merging of two co-flowing pure turbulent plumes with sources at the same level must be described solely in terms of the buoyancy flux of each plume and the horizontal separation of their origins. Thus the problem is completely specified by the buoyancy fluxes $\hat{F}_1$ and $\hat{F}_2$ (with $\hat{F}_1 \geqslant \hat{F}_2$ by convention) and the source separation χ_0 (see figure 1). Values for distances, such as the height at which the plumes merge and the location of the virtual origin of the resulting single plume, must be functions only of these three parameters.

Taking the height z_m at which the plumes might be considered merged as an example, one can write on dimensional grounds

$$\frac{z_m}{\chi_0} = func\left(\frac{\hat{F}_2}{\hat{F}_1}\right). \tag{2.1}$$

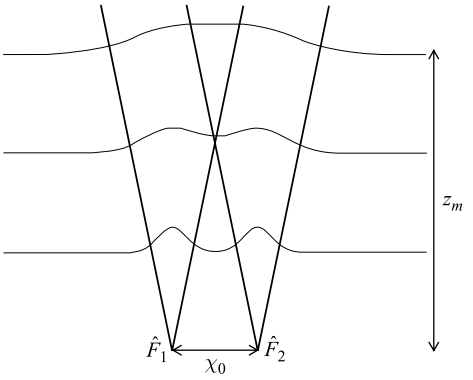

FIGURE 1. Schematic of two equal turbulent plumes showing the coalescence of the mean buoyancy profiles and the height z_m of merging. Note that the plumes are assumed to have the same source height.

Therefore the coalescence height scales linearly on the separation and is an unknown function of the ratio of the buoyancy fluxes. This differs from the laminar case where z_m is scaled on the square of the separation (see (1.1)).

Throughout the rest of this paper the following dimensionless variables will be used:

$$\lambda = \frac{z}{\chi_0}, \quad \phi = \frac{\chi}{\chi_0}, \quad \gamma = \frac{b}{\chi}, \tag{2.2}$$

where b is the plume radius and z is the height above the plume sources.† The variable χ is the separation of the plume axes at any given height. It should be noted that γ is the ratio of the local plume radius to the local axial separation, not to the initial separation. The ratio of the buoyancy fluxes is denoted by

$$\psi = \frac{\hat{F}_2}{\hat{F}_1} \leqslant 1. \tag{2.3}$$

Finally, the subscript m denotes the value of a variable at the point where the plumes merge, and the subscript ub means an upper bound on that value.

2.1. *Equal plumes*

Consider first the simplest case of two equal plumes ($\psi = 1$) with origins at the same height. A simple model, in which the plumes do not interact as they coalesce, provides a limit on λ_m. The average buoyancy profile of a single turbulent plume can be taken as Gaussian, with a radius given by $6\alpha z/5$, where α is the entrainment constant (Morton, Taylor & Turner 1956). Allowing the two Gaussians to grow into each other as the height increases, and to have no other effect on each other, leads to a buoyancy profile function of the form

$$g'(r, z) \sim f(z)E(r), \tag{2.4}$$

† Throughout this paper we use the term 'merging height' to mean the vertical distance from the plume sources to the point at which they are considered merged. This term is used for convenience, though it should be noted that for negatively buoyant plumes the 'height' will be the distance below the plume sources.

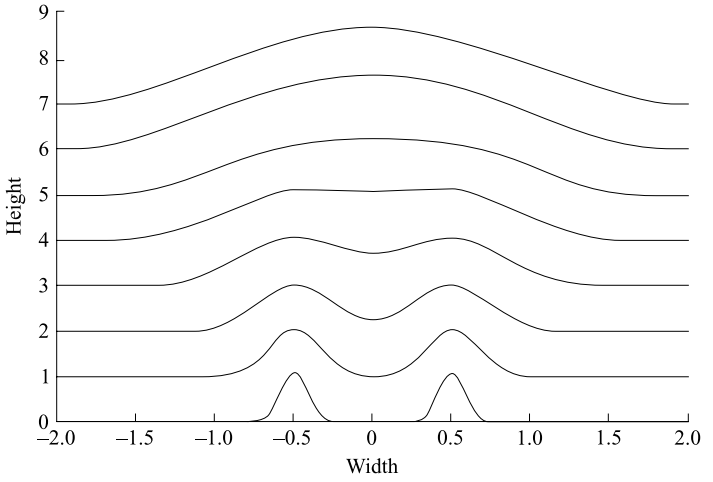

FIGURE 2. Merging Gaussian functions for a unit source separation.

where $E(r)$ is given by

$$E(r) = \left(\exp\left[-\left(r - \tfrac{1}{2}\chi_0\right)^2/b^2\right] + \exp\left[-\left(r + \tfrac{1}{2}\chi_0\right)^2/b^2\right]\right), \tag{2.5}$$

where r is the radial distance from the plume axis and g' is the reduced gravity. The model of Bjorn & Nielsen (1995) is similar, except that they were concerned with the velocity profiles. Their model is identical to the present case for equal plumes, though when $\psi < 1$ the ratio of the profile heights will differ. Here the buoyancy rather than the velocity profile is used to judge whether plumes have merged, because the buoyancy is the driving force, and once the driving force can be considered a single entity, it is reasonable to assume that the flow will behave as a single entity. For the case of equal turbulent plumes the choice between buoyancy and velocity profiles will make no difference as they will both merge at the same height. However for unequal plumes the ratio of the peak velocities will be $\psi^{1/3}$, whereas the ratio of the peak buoyancies will be $\psi^{2/3}$.

This function (2.4) is plotted in figure 2 for $1 < \lambda < 8$ and $\chi_0 = 1$. Clearly the two Gaussians coalesce when λ is large enough, but it is difficult to say where the plumes can be said to have merged. We define the merging height to be the height at which the centreline value first becomes a local maximum – in other words, the height at which there are no longer two distinct peaks. This condition can be written as

$$\frac{\mathrm{d}^2 E}{\mathrm{d}r^2} = 0 \quad \text{at} \quad r = 0, \tag{2.6}$$

and, for non-interacting plumes, is easily solved to give

$$\chi_0 = \sqrt{2b} \quad \text{or} \quad \gamma_m = \frac{1}{\sqrt{2}}. \tag{2.7}$$

In terms of the non-dimensional height one obtains

$$\lambda = \lambda_{ub} = \frac{1}{\sqrt{2}}\frac{5}{6\alpha}, \tag{2.8}$$

as an upper bound on λ_m. For an entrainment constant $\alpha = 0.09$, (2.8) gives $\lambda_{ub} = 6.5$. We will discuss the choice of the numerical value of α in § 4.

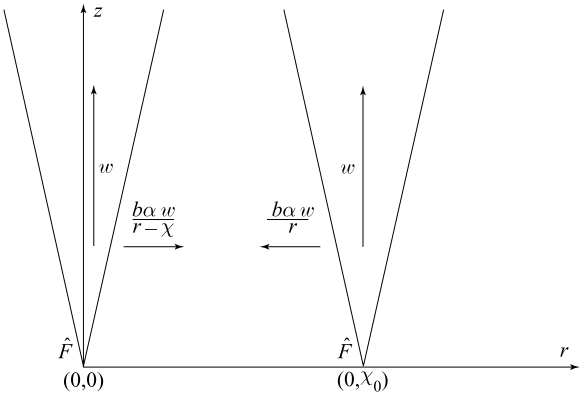

FIGURE 3. Schematic of two equal turbulent plumes showing the vertical plume velocity and the deflection velocity due to the other plume's entrainment.

As shown earlier (Bjorn & Nielsen 1995) this estimate of λ_m is poor, as it assumes that the plumes do not interact but simply merge together as they grow laterally. In order to model the drawing together of two equal plumes we need to consider the entrainment of one plume by another.

Based on experimental results (for example, Rouse, Yih & Humphreys 1952) it is reasonable to take the velocity field outside the plumes created by entrainment as horizontal. The mean entrainment velocity field, over a horizontal plane across the two plumes, may be approximated by two sinks of strength $-m(z)$ placed at $(0, 0)$ and $(0, \chi)$. The complex velocity potential in this horizontal plane is given by

$$\Omega = -\frac{m}{2\pi}(\ln(Z) + \ln(Z-\chi)), \tag{2.9}$$

where Z is the complex variable $r\,\mathrm{e}^{\mathrm{i}\theta}$. The velocity field is given by

$$U = \frac{\partial \Omega}{\partial Z} = -\frac{m}{2\pi}\left(\frac{1}{Z} + \frac{1}{(Z-\chi)}\right). \tag{2.10}$$

The sink strength of the plume is

$$m = \int_0^{2\pi} b\alpha w \,\mathrm{d}\theta, \tag{2.11}$$

or

$$\frac{m}{2\pi} = b\alpha w. \tag{2.12}$$

Along the line joining the sources of the plumes ($\theta = 0$) the velocity is given by

$$U_{\theta=0} = -b\alpha w\left(\frac{1}{r} + \frac{1}{r-\chi}\right). \tag{2.13}$$

A schematic of two plumes showing the deflection velocity of each due to the other plume is shown in figure 3. The above velocity field can be used to calculate the deflection of the plume from the vertical at any given height. This deflection can be integrated from the plume source to the point of coalescence to give a more accurate estimate of λ_m. Along each plume centreline the value of the horizontal entrainment velocity due to that plume is zero, and only the term resulting from the second plume need be considered. In fact (2.13) leads to a singularity at $r = 0$, but as the expression

is valid only outside the plume creating the flow, this singularity can be ignored. The validity of the assumption that the fields can be added is questionable, but Gaskin, Papps & Wood (1995) showed experimentally that, for ambient velocities of the same order as the entrainment velocity, the two fields could be added, and this result will be used below. Furthermore, the entrainment flow into the sink is irrotational and governed by Laplace's equation, and the linearity of this equation justifies the addition of the two fields.

Simplifying (2.13) gives an expression for the mean horizontal velocity u on the axis

$$u = -\frac{b\alpha w}{\chi}. \tag{2.14}$$

Assuming that each plume is passively advected by the entrainment field of the other, the rate of change of separation with height will be given by the ratio of the vertical to the horizontal velocities at the plume axis (figure 3). As both plumes are deflected equally, the full expression can be simplified to

$$\frac{\mathrm{d}\chi}{\mathrm{d}z} = -2\frac{1}{w}\frac{\alpha w b}{\chi}. \tag{2.15}$$

Substituting $b = 6\alpha z/5$, $\lambda = z/\chi_0$ and $\phi = \chi/\chi_0$ gives

$$\frac{\mathrm{d}\phi}{\mathrm{d}\lambda} = -\frac{12\alpha^2}{5}\frac{\lambda}{\phi}, \tag{2.16}$$

which can be integrated to give

$$\phi^2 - \phi_0^2 = \frac{12\alpha^2}{5}\left(\lambda_0^2 - \lambda^2\right), \tag{2.17}$$

where $\phi_0 = 1$ and $\lambda_0 = 0$. From (2.6) we find

$$\phi_m = \frac{1}{\gamma_m}\frac{6\alpha}{5}\lambda_m. \tag{2.18}$$

From (2.7) we have $\gamma_m = 1/\sqrt{2}$, the value of λ_m is therefore given by

$$\lambda_m = \frac{1}{\alpha}\sqrt{\frac{25}{132}}. \tag{2.19}$$

Note that the use of $\gamma_m = 1/\sqrt{2}$ derived for the non-interacting model is appropriate here as the correction for the drawing together of the plumes assumes that they are passively advected only. The radial growth rate of each plume is assumed to be unaffected by this process.

For an entrainment constant $\alpha = 0.09$, $\lambda_m = 4.8$ or approximately 2/3 of the upper bound placed on the merger height by assuming no interaction (see (2.8)). This value considerably exceeds the value of around 1 that is observed for turbulent line plumes. This difference suggests that axisymmetric plumes merge further from the plume sources than line plumes, as expected.

2.2. *Unequal plumes*

For plumes of unequal buoyancy flux, the first key factor is the lack of symmetry. The buoyancy profiles of the two plumes have different magnitudes, with the peaks scaling on $\hat{F}^{2/3}$. The weaker plume will also have a lower velocity, with its peak velocity scaling on $\hat{F}^{1/3}$. For this case, the equivalent expression to (2.4) is

$$g'(r, z) \sim f(z)E(r, \psi). \tag{2.20}$$

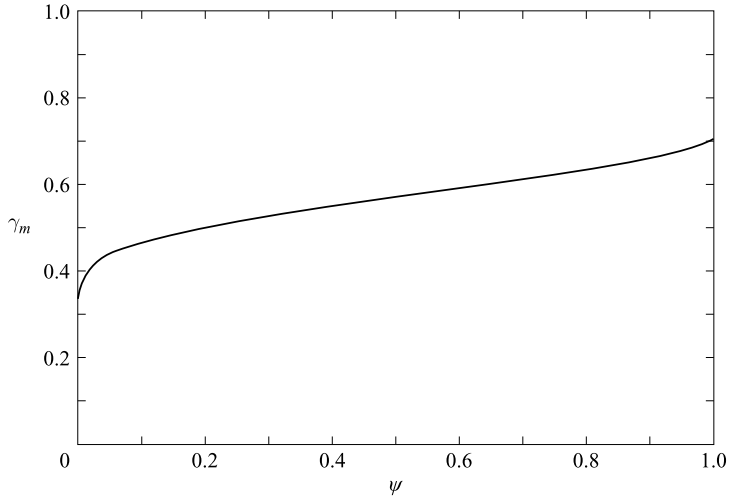

FIGURE 4. Plume radius for the merger of two unequal plumes, plotted as a function of the buoyancy flux ratio.

where for unequal plumes, $E(r)$ is given by

$$E(r,\psi) = \left(\exp\left[-\left(r-\tfrac{1}{2}\chi_0\right)^2/b^2\right] + \psi^{2/3}\exp\left[-\left(r+\tfrac{1}{2}\chi_0\right)^2/b^2\right]\right)$$
$$= \left(\exp[-(r/b-1/2\gamma)^2] + \psi^{2/3}\exp[-(r/b+1/2\gamma)^2]\right). \tag{2.21}$$

Clearly, the occurrence of a buoyancy peak on the centreline is no longer an appropriate criterion for coalescence. The obvious equivalent definition is the point when the trough in the combined profile disappears, i.e.

$$\frac{\mathrm{d}E}{\mathrm{d}r} = 0, \quad \frac{\mathrm{d}^2E}{\mathrm{d}r^2} = 0. \tag{2.22}$$

This gives the same result as (2.6) in the limit as $\psi \to 1$.

For a given ψ this criterion will only be satisfied once over all (r, b, γ). A numerical search was used to find the values of $\gamma_m(\psi)$ that satisfy (2.22). Figure 4 shows the results of this search. The upper bound on the coalescence height is given by $\lambda_{ub} = 5\gamma_m/(6\alpha)$.

From the entrainment velocity field, noting that the velocity scales on $\hat{F}^{1/3}$, we can derive the equivalent vector diagram, shown in figure 5. The weaker plume will be deflected more than the stronger plume, as is observed in laminar plumes and turbulent line plumes.

As before (see (2.15)) it is possible to write an expression for the rate of change of separation with height:

$$\frac{\mathrm{d}\chi}{\mathrm{d}z} = \alpha\left(\psi^{1/3} + \psi^{-1/3}\right)\frac{b}{\chi}, \tag{2.23}$$

which can be written as

$$\frac{\mathrm{d}\phi}{\mathrm{d}\lambda} = \frac{6\alpha^2}{5}\left(\psi^{1/3} + \psi^{-1/3}\right)\frac{\lambda}{\phi}. \tag{2.24}$$

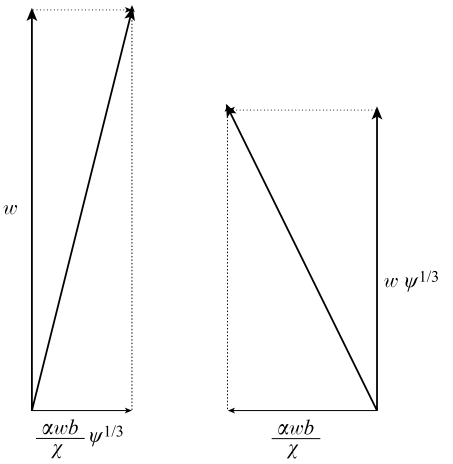

FIGURE 5. Vector diagram showing the merging velocities for two unequal plumes.

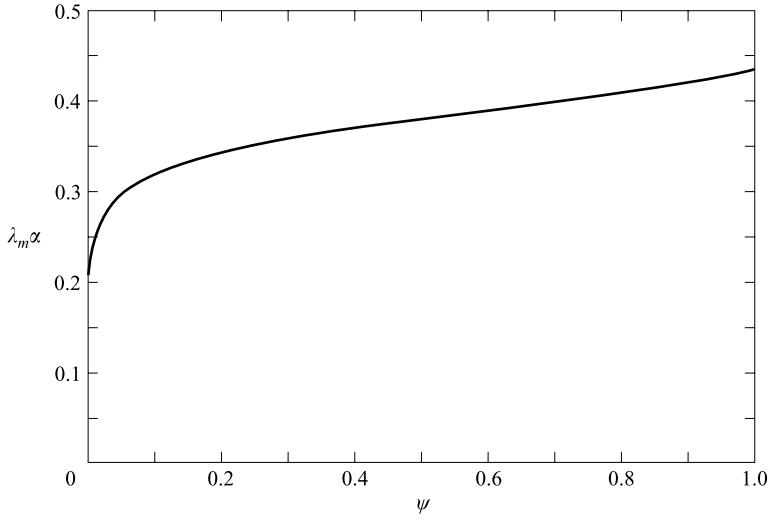

FIGURE 6. Merging height $\lambda_m\alpha$ for unequal turbulent plumes, plotted as a function of the ratio of the buoyancy fluxes.

Again $\phi_0 = 1$ and $\lambda_0 = 0$. The full expression for λ_m is

$$\lambda_m = \frac{1}{\alpha}\sqrt{\frac{5}{6}}\frac{1}{\sqrt{6/(5\gamma_m^2) + \psi^{1/3} + \psi^{-1/3}}}. \tag{2.25}$$

Using values for γ_m from figure 4, it is possible to calculate $\lambda_m\alpha$. Values for this expression are plotted in figure 6. Note that for $\psi = 1$ $\gamma_m = 1/\sqrt{2}$ and (2.25) becomes

$$\lambda_m\alpha = \sqrt{\frac{5}{6}}\frac{1}{\sqrt{12/5 + 1 + 1}} = \sqrt{\frac{25}{132}}, \tag{2.26}$$

giving the same result as for equal plumes (2.19).

A number of key points emerge in figure 6. First, λ_m varies only weakly over a wide range of ψ, with only about a 25% variation for $0.15 < \psi < 1$ and with a very

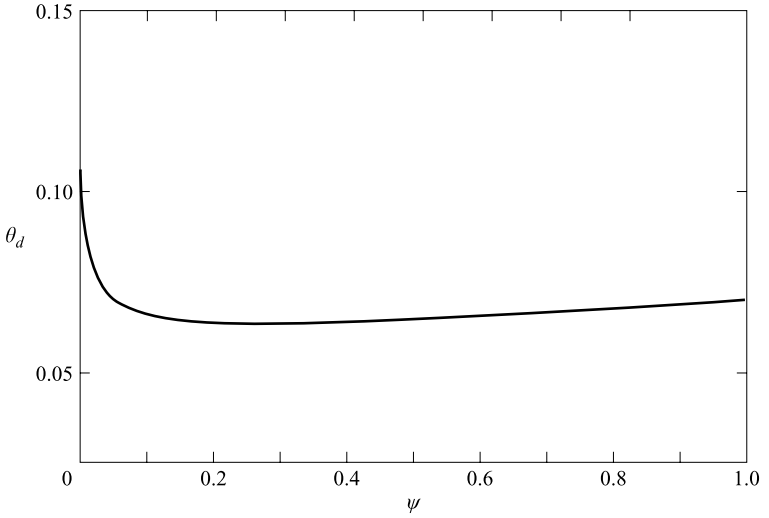

FIGURE 7. Total angular deflection as a function of the buoyancy flux ratio.

sharp drop off below 0.15. Second, the estimate of λ_m given by the advection model is about $0.6\lambda_{ub}$ to $0.7\lambda_{ub}$. Thus, although advection by the entrainment field is weaker than in line plumes, it is still a substantial process. Finally, (2.25) indicates that λ_m is inversely proportional to α (recall that γ_m is independent of α). Thus the predicted value of λ_m will vary significantly, depending on the choice of entrainment coefficient.

One remaining question is whether, having corrected for the drawing together of the plumes, it is worth recalculating the plume entrainment field based on the angle of deflection of the plumes. The calculation of z_m could then be repeated. This exercise would only be worthwhile if the plumes were deflected significantly from the vertical. The greatest angular deflection occurs for small ψ where the weaker plume is deflected considerably more than the stronger. The final total deflection of the two plumes is equal to the initial separation minus the final separation ($\phi_d = 1 - \phi_m$). Assuming, for small ψ, that only one plume is deflected, the total angular deflection will be approximately

$$\theta_d = \frac{1-\phi_m}{\lambda_m} = \frac{1}{\lambda_m} - \frac{6\alpha}{5\gamma_m}. \tag{2.27}$$

A plot of θ_d is shown in figure 7. It can be seen that even for values of ψ as low as 0.05 the total deflection is very small, and there is no need to recalculate the entrainment field.

3. The merged plume

A model was presented in § 2 to calculate the rate at which plumes coalesce. This section examines what happens once they have merged. As a first approximation it is assumed that, before coalescence, each plume has little effect on the bulk properties of the other, and that after coalescence the two plumes behave as a single axisymmetric plume. For example, it is assumed that the volume flux in each plume increases as it would if the other plume were not present, up until the point at which they have merged. This is a reasonable assumption, as Baines (1983) observed that for merging equal plumes the transition in behaviour from that of two separate plumes to a single plume occurs over a distance considerably smaller than the distance at which the two

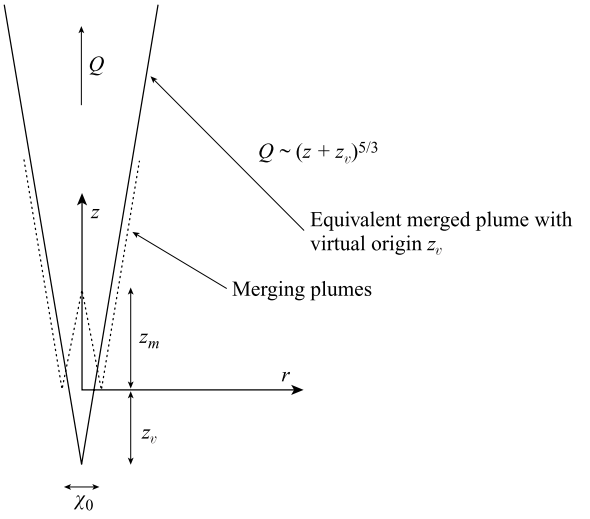

FIGURE 8. Schematic of two merging plumes showing far field and virtual origin.

plumes come together (a phenomenon that is also observed in experiments performed for this paper). Baines also notes that, although the bulk properties of the plume are as for a pure plume, the cross sectional area is not circular at the point of merger and undergoes a transition to axisymmetry over a greater distance. No attempt is made to model this cross-sectional transition in this paper as it appears to have little effect on the bulk flow properties. This is in keeping with the history of the use of the entrainment assumption and the entrainment equations of Morton *et al.* (1956). Although the entrainment assumption requires strict self-similarity for its derivation it is found to be a remarkably effective model in quasi-similar situations such as a plume in a stratified environment.

Here we establish the far-field behaviour of the single plume that forms from the combination of two plumes. As the buoyancy flux of the single plume is the sum of the buoyancy fluxes of the two source plumes (in an unstratified environment), the parameters that need to be established are the volume and momentum fluxes. In the far field the flow will behave as a pure plume, so the fluxes can be written in terms of the buoyancy flux of that plume (which is known) and a height. The problem, therefore, reduces to establishing the point from which the height is measured, that is, the location of the virtual origin of the resulting plume. This problem is shown schematically in figure 8.

3.1. *Equal plumes*

Again we start with the simplest case of two equal plumes. Hunt & Kaye (2001) showed that the location of the virtual origin of a general plume was a function of the source conditions of buoyancy flux, momentum flux and volume flux ($\hat{F}_0$, $\hat{M}_0$, $\hat{Q}_0$). For consistency we use the following variables

$$M = \frac{2\hat{M}}{\pi}, \quad F = \frac{2\hat{F}}{\pi}, \quad Q = \frac{\hat{Q}}{\pi}. \tag{3.1}$$

These conditions can be used to determine the effective source radius

$$b_0 = \frac{Q_0}{M_0^{1/2}} \tag{3.2}$$

and the source Froude number

$$\Gamma = \frac{5Q_0^2F_0}{4\alpha M_0^{5/2}}. \tag{3.3}$$

The location of the virtual origin can be calculated by evaluating the fluxes of buoyancy, volume and momentum in the plume at some point after the plumes have merged.

Assuming that the plumes act independently up to the merging height and behave as a single axisymmetric plume after that height, we may add together the volume and momentum fluxes of the two source plumes. The values for the single plume at the point of merging are given by

$$Q_m = 2\left(\frac{5F}{4\alpha}\right)^{1/3}\left(\frac{6\alpha\lambda_m\chi_0}{5}\right)^{5/3}, \tag{3.4}$$

$$M_m = 2\left(\frac{5F}{4\alpha}\right)^{2/3}\left(\frac{6\alpha\lambda_m\chi_0}{5}\right)^{4/3} \tag{3.5}$$

and

$$F_m = 2F. \tag{3.6}$$

Buoyancy and volume flux must be conserved as no fluid is observed to detrain from the plumes, and the momentum flux is conserved as no external force acts on the flow as a result of the merging process.

Using these values, it is possible to establish the values of Γ_m and b_m.

$$\Gamma_m = \sqrt{2}, \quad b_m = \frac{6\alpha}{5}\lambda_m\chi_0\sqrt{2}. \tag{3.7}$$

Hunt & Kaye (2001) showed that the distance of virtual origin below the plume source is

$$z^*_{avs} = \Gamma^{-1/5}(1-\delta) \tag{3.8}$$

where

$$z^* = \frac{z}{(5/6\alpha)\left(Q_0/M_0^{1/2}\right)}, \tag{3.9}$$

and δ is given by (35) from Hunt & Kaye (2001).

This gives a value for the distance to the virtual origin, relative to the individual plume origins, of

$$z_v \approx 0.91\sqrt{2}\lambda_m\chi_0 - \lambda_m\chi_0. \tag{3.10}$$

Scaling the height on the initial plume separation χ_0 and using the value of $\lambda_m\alpha = 0.435$ from (2.19), the location of the virtual origin for the resulting merged plume is

$$\frac{z_v}{\chi_0} \approx \frac{0.124}{\alpha}. \tag{3.11}$$

For $\alpha = 0.09$ the value becomes $z_v/\chi_0 = 1.37$. Thus, when two equal plumes merge to form a single plume, the virtual origin of that plume will be approximately 1.37 plume separations below the origins of the two constituent plumes. This, however, is only the simplest case; it is important to look also at the case of unequal interacting plumes.

It is worth noting that at the point of merger $\Gamma > 1$ and, therefore, the plume is lazy (as opposed to forced). Little work has been done on the topic of lazy plumes near

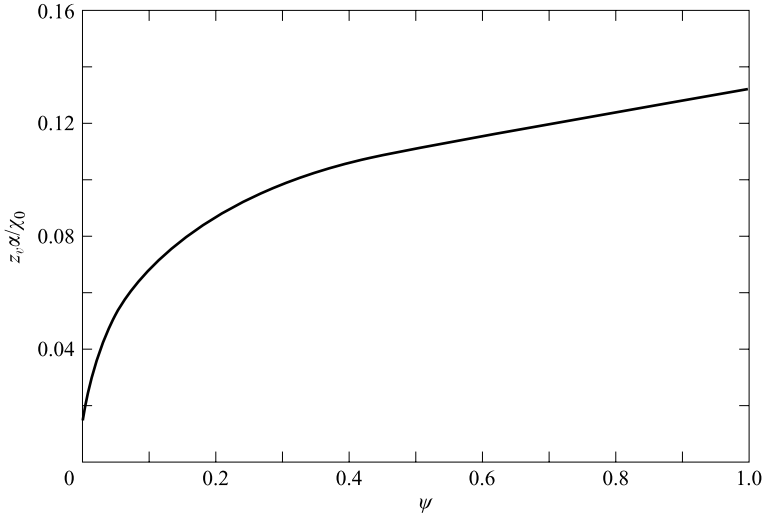

FIGURE 9. Virtual origin location for a plume formed by two merging plumes, plotted as a function of the buoyancy flux ratio.

their source. However, lazy plumes can contract (see figure 5 of Morton & Middleton 1973). It is likely that this contraction during the adjustment from lazy to pure plume is partly responsible for the observation of vertical sides to the merged plume made by Baines (1983) and the authors of this paper.

3.2. *Unequal plumes*

For unequal plumes, again assuming that the plumes act independently up to the point at which they coalesce, (3.4), (3.5) and (3.6) become

$$Q_m = \left(1+\psi^{1/3}\right)\left(\frac{5F_1}{4\alpha}\right)^{1/3}\left(\frac{6\alpha\lambda_m\chi_0}{5}\right)^{5/3}, \tag{3.12}$$

$$M_m = \left(1+\psi^{2/3}\right)\left(\frac{5F_1}{4\alpha}\right)^{2/3}\left(\frac{6\alpha\lambda_m\chi_0}{5}\right)^{4/3} \tag{3.13}$$

and

$$F_m = (1+\psi)F_1. \tag{3.14}$$

This yields values for Γ and b of

$$\Gamma_m = \frac{(1+\psi)\left(1+\psi^{1/3}\right)^2}{\left(1+\psi^{2/3}\right)^{5/2}} \tag{3.15}$$

and

$$b_m = \left(\frac{6\alpha}{5}\right)\frac{\left(1+\psi^{1/3}\right)}{\left(1+\psi^{2/3}\right)^{1/2}}\lambda_m\chi_0. \tag{3.16}$$

With these expressions and the values plotted in figure 6, we calculate the location of the virtual origin, which is plotted in figure 9. Again there is only a small variation in the location of the virtual origin over a wide range of ψ, because the dominant terms in calculating the virtual origin are the volume and momentum flux, both of which are weak functions of the buoyancy flux and, therefore, of ψ.

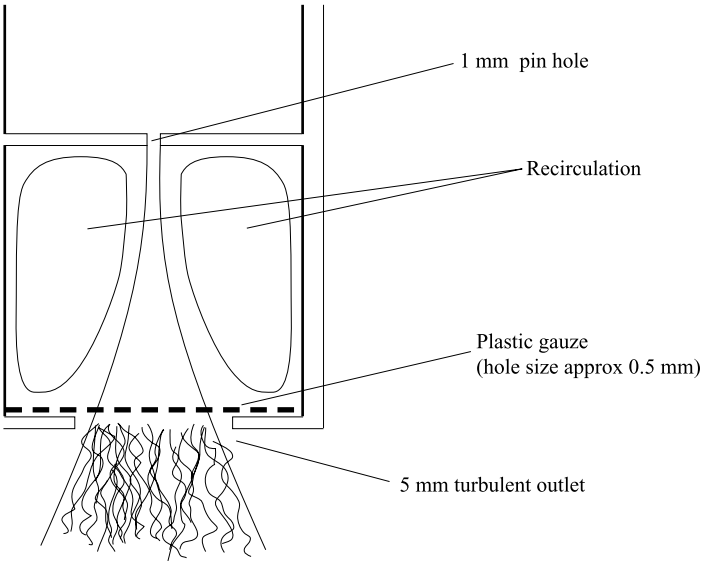

FIGURE 10. Schematic diagram of the Cooper plume nozzle used to produce a turbulent plume source.

4. Experiments

Sections 2 and 3 describe theoretical predictions for the merging height of co-flowing turbulent plumes, and the behaviour of the resulting plume in the far field. Experiments have been performed to test the validity of these models. The experiments were carried out using salt plumes in water. The density of the salt solution and the flow rate determined the buoyancy flux. These were chosen such that the plumes were close to ideal, i.e. with small initial volume and momentum fluxes. Corrections for the non-ideal nature of the sources were made by calculating the virtual origin z_v using the method described in Hunt & Kaye (2001). These corrections were typically of the order of 1 cm, which is considerably less that the typical coalescence heights measured of 10–30 cm. For the case of unequal plumes, the average of the two virtual origin corrections was used. The difference between the origin corrections for each separate plume was typically less than 0.5 cm, or 10% of the plume separation, making the use of the average correction a reasonable approximation.

Typical flow rates used in the experiments were between 0.5 and 2.5 $\mathrm{cm^3\,s^{-1}}$. The source buoyancy was varied between 30 and 150 $\mathrm{cm\,s^{-2}}$. The equal plume experiments were run using the dye attenuation technique in a glass tank approximately 60 cm square with a depth of 180 cm. The unequal plume experiments were run using a light-induced fluorescence (LIF) technique in a 64 cm square Perspex tank that was filled to a depth of 15–35 cm. In order to maintain a turbulent plume from the source, a special nozzle was constructed.† Figure 10 shows a schematic of the nozzle used. The nozzle allowed the creation of a turbulent outlet that would normally be laminar at the flow rates used. Figure 7 of Hunt & Linden (2001) shows the outflow from this nozzle compared to a standard cylindrical tube. The use of the Cooper nozzle meant that the plumes rapidly developed into their self-similar form. This can be more

† The initial nozzle was designed by Dr Paul Cooper, Department of Mechanical Engineering, University of Wollongong, NSW, Australia.

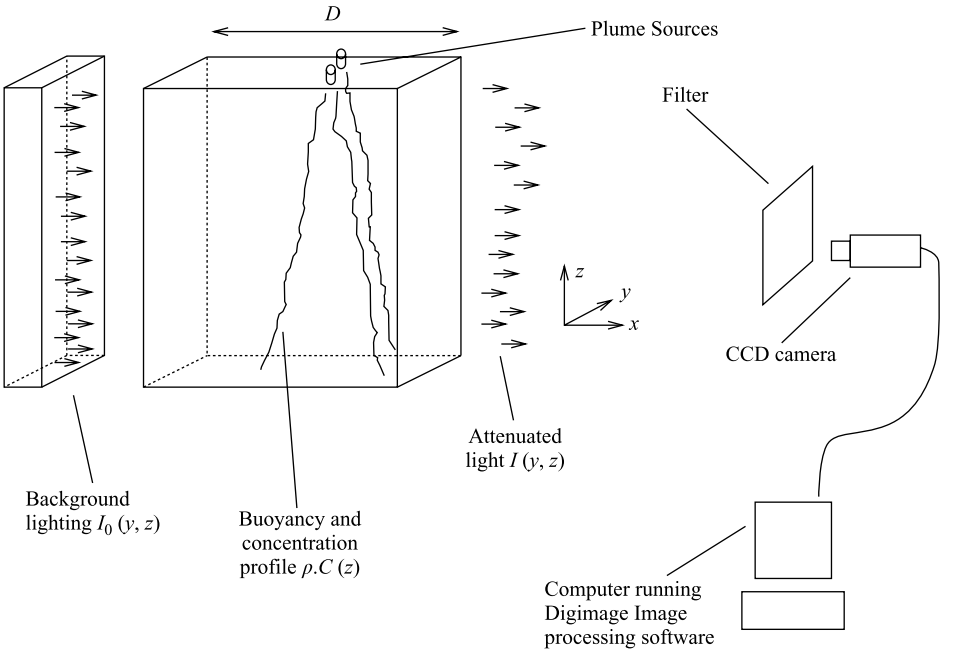

FIGURE 11. Schematic showing the experimental setup for measuring buoyancy with an attenuating dye such as potassium permanganate.

clearly seen in figure 13 below, which shows time-averaged buoyancy profiles from an experiment where two equal plumes coalesce. Clearly the profiles are Gaussian in nature well before they coalesce.

4.1. *Merging height*

The first set of experiments performed was designed to determine the merging height given by the condition defined in (2.20), for both equal and unequal plumes. In order to measure this height, buoyancy profiles needed to be measured. The experiments conducted for this paper used two different techniques for this purpose: a dye attenuation technique and a light-induced fluorescence (LIF) technique.

4.1.1. *Experimental techniques*

The principle behind the dye attenuation method is that the attenuation of the light across a dyed region is a function of the initial light intensity, the local dye concentration, and the region depth. This technique uses small concentrations of dye that acts as a passive tracer for the salt concentration. The accuracy relies on the fact that the diffusion rate of the dye is of a similar order to the diffusion rate of the salt that creates the buoyant plume, and that this rate is significantly smaller than turbulent diffusion in the plume. In the experiments presented here typical Péclet numbers were of the order of 10^5 for both the salt and dye solutions, implying that molecular diffusion is negligible.

The attenuation relationship for light passing through a dye solution is given by

$$\frac{\mathrm{d}I(x, y, z)}{\mathrm{d}x} \sim -f(c(x, y, z))I(x, y, z), \tag{4.1}$$

where x is the direction between the light source and the camera (shown in figure 11). For any given light frequency and for small dye concentrations c, the function f

is approximately linear in c. By using a filter in front of the camera it is possible to narrow the band of frequencies observed, thus making the function more linear. For example, potassium permanganate solution with a green filter gives a very linear response for concentrations up to $0.1\,\mathrm{g\,l^{-1}}$ (see Cenedese & Dalziel 1998 for a more detailed description of the technique).

Assuming that the buoyancy is a linear function of the dye, the attenuation across the depth of the tank at any point in the (y, z)-plane is

$$\frac{\mathrm{d}I}{\mathrm{d}x} = -\sigma g'(x) I. \tag{4.1}$$

For a distribution of g' of the form (2.4), we can integrate (4.1) to give

$$\ln\left(\frac{I}{I_0}\right) \sim -\sigma f(z) \int_{-\infty}^{\infty} \left(\exp\left[-x^2 + \left(y - \tfrac{1}{2}\chi_0\right)^2/b^2\right] + \exp\left[-x^2 + \left(y + \tfrac{1}{2}\chi_0\right)^2/b^2\right]\right) \mathrm{d}x, \tag{4.2}$$

Taking the y-axis aligned with the two plume sources and the x-axis as the horizontal direction along the light path (see figure 11), then (4.2) can be re-written as

$$\ln\left(\frac{I}{I_0}\right) \sim -\sigma f(z)\left(\exp\left[-\left(y - \tfrac{1}{2}\chi_0\right)^2/b^2\right] + \exp\left[-\left(y + \tfrac{1}{2}\chi_0\right)^2/b^2\right]\right) \times \int_{-\infty}^{\infty} \exp(-x^2/b^2)\,\mathrm{d}x \sim CE(y, \chi_0, b), \tag{4.3}$$

where C is a constant. Thus, the logarithm of the attenuation of the light as it passes through the plumes is a function of the same form as (2.4). The merging height can then be established by looking for the height in the image at which the buoyancy peak first appears on the centreline. In fact, it is not even necessary to establish the value of C. Intensity measurements and image manipulation were all done using the image processing software Digimage.† Images were recorded and then averaged over a period of one minute. The averaging time of one minute was sufficiently long to give a smooth mean buoyancy profile, but it was not possible to average for longer as the tank used for the experiment began to fill up with plume fluid.

Light-induced fluorescence techniques involve shining a thin light sheet through a plume dyed with a fluorescent dye such as sodium fluorescein and observing the plume perpendicular to the light sheet. Using this technique it is possible to establish the mean concentration of the dye, and therefore the buoyancy of the plume. A schematic of the experimental setup is shown in figure 12. It is again necessary that the dye and salt diffuse at a similar rate, considerably slower than that caused by the turbulent mixing of the plume. It is assumed that the amount of light observed at a point is linearly proportional to the intensity of the light sheet and the dye concentration,

$$I_f = AcI_0, \tag{4.4}$$

where $A = \mathrm{const}$. Finally, it is assumed that the light sheet attenuation is linearly proportional to the local intensity and local dye concentration

$$\frac{\mathrm{d}I_0}{\mathrm{d}\gamma} = -BcI_0, \tag{4.5}$$

where $B = \mathrm{const}$. By taking an image of a uniform concentration of fluorescein it is possible to establish both the rate A of fluorescence and the rate B of attenuation of the light sheet. For more details of this technique, see Dalziel, Linden & Youngs

† http://www.damtp.cam.ac.uk/user/fdl/people/sd/digimage/document/index.htm

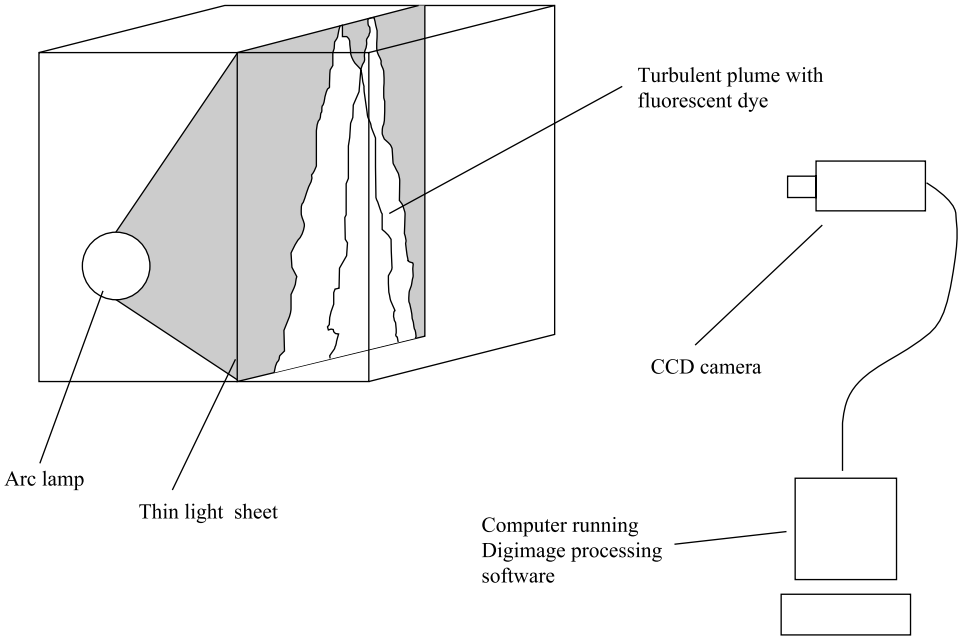

FIGURE 12. Schematic showing the experimental setup for measuring buoyancy with a fluorescent dye such as sodium fluorescein.

(1997). Again the plume image was averaged over a period of around one minute, the coalescence height was measured using Digimage, and this height was corrected for the virtual origin of the source plumes. After processing by Digimage both the dye attenuation and LIF techniques produce the same profile information.

4.1.2. *Experimental results*

(i) *Equal plumes*

Experiments were conducted with different initial axial separations from 2.5 cm to 7.5 cm to establish the merging height. Figure 13 shows an example of the profiles for two equal plumes. The figure illustrates the fully developed plumes coalescing, with the two plumes merging at $\lambda \approx 4.5$. Figure 14 gives the results of the measurements of the coalescence height. A straight line was fitted through the points. The line is a least-squares fit that was not forced through the origin. The slope of the straight line is the value of λ_m, see (2.2). The value of λ_m based on these experiments is $\lambda_{me} = 4.1 \pm 0.25$. For $\alpha = 0.09$ and the theoretical prediction $\alpha\lambda_m = 0.44$ we obtain $\lambda_{mt} = 4.8$ which is larger than the measured value, implying that the plumes coalesce closer to the source than predicted. A discussion of possible reasons for this discrepancy is presented later.

(ii) *Unequal plumes*

The unequal plume experiments were all conducted at a fixed separation of 5 cm. The results for this case are plotted in figure 15 as values of λ_m plotted against ψ. The theoretical predictions for λ_m and the upper bound λ_{ub} for $\alpha = 0.09$, as well as λ_m for $\alpha = 0.1$, are also shown in figure 14. It is clear that the theory consistently over-predicts the measured coalescence height. However, the function is very similar to the predictions, with very little variation in λ_m over the range $0.3 < \psi < 1$.

There are various reasons for the discrepancy between the theoretical and predicted heights. The predicted merging height is very sensitive to the value of α. As shown

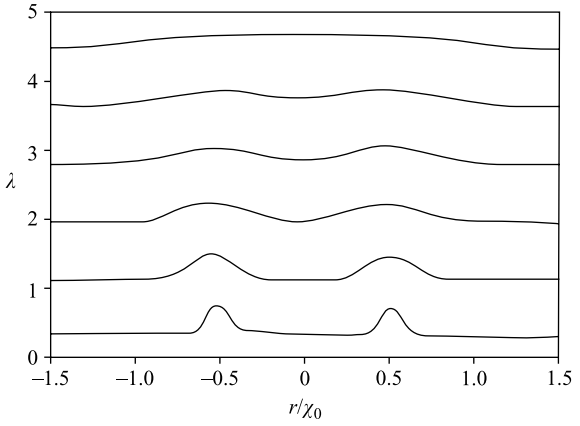

FIGURE 13. Buoyancy profiles for two equal plumes showing their Gaussian profiles prior to merging, and the gradual coalescence. The profiles were measured using the dye attenuation technique.

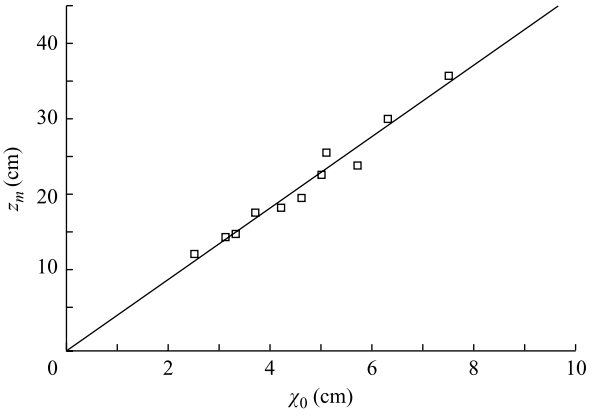

FIGURE 14. Plume merging height for equal plumes plotted against initial separation.

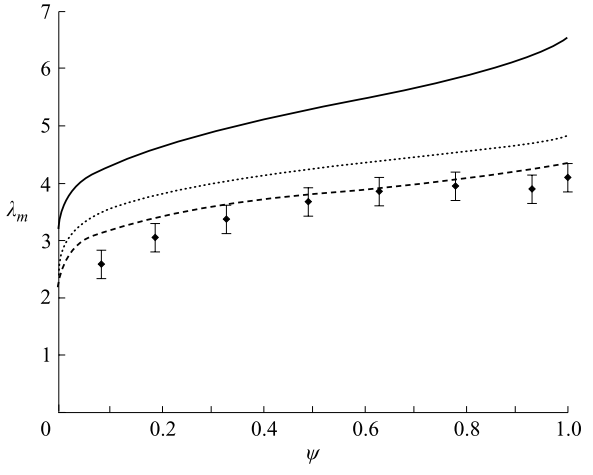

FIGURE 15. Plume merging height plotted as a function of the buoyancy flux ratio. The lines plotted are the theoretical predictions for $\lambda_{ub}(\alpha = 0.09)$, $\lambda_m(\alpha = 0.09)$ and $\lambda_m(\alpha = 0.1)$ (top to bottom).

in figure 15, using a value of $\alpha = 0.1$ brings the theoretical prediction within the experimental error for the majority of measurements.

At this stage it is worth reviewing the most appropriate value of α for this study. The literature is inconclusive. When direct velocity and temperature measurements are made the entrainment rate derived from the profile radius has an average value of α just over 0.1 (see Rouse *et al.* 1952; George, Alpert & Tamanini 1977; Nakagoma & Hirata 1977; Chen & Rodi 1980; Papanicolaou & List 1988; Shabbir & George 1994). When the entrainment rate is determined by either direct or indirect flow rate measurements or other results based on the entrainment model of Morton *et al.* (1956) the average value is 0.088 (see Baines 1983; Baines & Turner 1969; Morton *et al.* 1956; Turner 1986). It might, therefore, be reasonable to suggest that one value of α (based on the measured plume profiles) be used for the merging process and a second (based on flow rate measurements) be used for calculating the far-field flow, but this is an inelegant idea. Instead, it is worth noting that the use of an entrainment coefficient is a turbulence closure whose numeric value is likely to have only order of magnitude significance when used beyond the scope for which it was measured. As a result this paper will present theoretical results independently of α where possible, and will use $\alpha = 0.09$ for experimental results except where otherwise stated.

For smaller values of ψ the difference between theory and experiment increases. For these lower values of ψ it was not always possible to have a fully developed turbulent outlet for the weaker source, and the discrepancy between the virtual origin heights of the two plumes is greatest. The buoyancy profile of the weaker plume is also approximately one fifth of that of the stronger plume for the lowest value of ψ measured. This large difference also increases the error in the measurement of λ_m.

The model does, however, account for over 80% of the reduction in merging height for $\alpha = 0.09$ over a wide range of ψ. This indicates that the approach of the two plumes due to entrainment is the main process involved in causing the plume to coalesce.

4.2. *Far-field flow*

The model presented in § 3.2 focuses on the far-field behaviour of the merged plumes, and predicts the virtual origin of the resulting combined plume. In order to test this model, a series of flow rate measurements were made in the merged plume, using the technique described in Baines (1983). The plume separation was varied from 1.0 to 7.5 cm, and the buoyancy flux ratio was varied from $\psi = 0.23$ to 1.0. At low values of ψ different initial buoyancy and flow rate values were used to obtain large differences in buoyancy flux. Therefore, in order to keep the virtual origin corrections similar for each plume, different source diameters were needed. As a result source diameters from 0.3 to 0.5 cm were used. The buoyancy flux was varied between $\hat{F} = 28$–$174\,\mathrm{cm}^4\,\mathrm{s}^{-3}$.

The technique of Baines (1983) involves creating a plume in a tank and then forcing a net volume flux of ambient fluid through the tank. The plume falls to the bottom of the tank (or rises to the top if positively buoyant plumes are used) and spreads out. This spreading flow creates a two-layer stratification that inhibits flow across the density interface. The layer formed by the plume outflow will grow in thickness until a steady state is reached where the volume flux through the tank matches the volume flux in the plume at the height of the density interface. By measuring the distance from the source to the interface and the flow rate through the tank one can measure the plume flow rate as a function of distance form the source. The interface height is varied by adjusting the flow rate through the tank.

The results are plotted in the form z/χ_0 against $Q^{3/5}F_1^{-1/5}/\chi_0$. They are consistent with Baines (1983); the only difference is that all distances are scaled on the initial

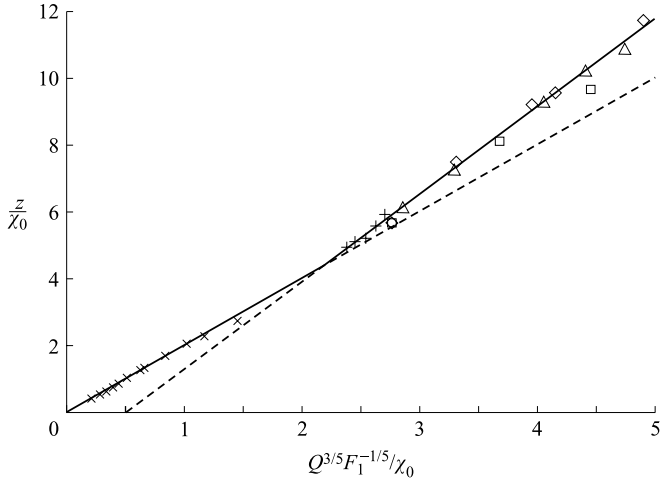

FIGURE 16. Flow rate measurements for two merging plumes of equal buoyancy flux $\psi = 1$: $\times$, $\hat{F}_1 = 174$, $\chi_0 = 2.5 - 7.5$; $+$, $\hat{F}_1 = 28$, $\chi_0 = 2.5$; $\square$, $\hat{F}_1 = 88$, $\chi_0 = 1.0$; $\triangle$, $\hat{F}_1 = 113$, $\chi_0 = 1.0$; $\diamond$, $\hat{F}_1 = 80$, $\chi_0 = 1.0$.

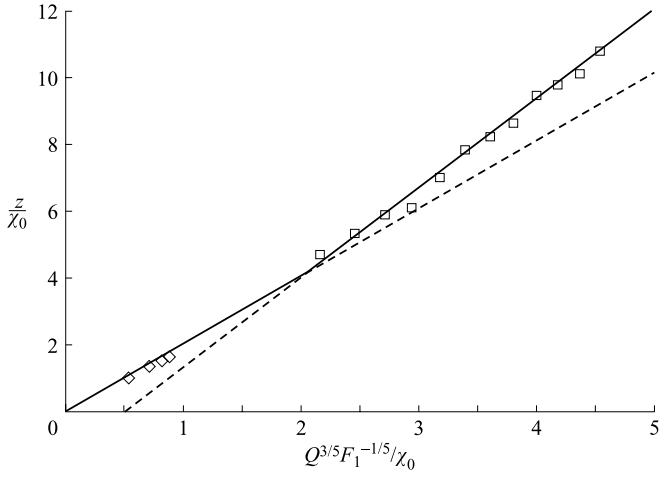

FIGURE 17. Flow rate measurements for two merging plumes of buoyancy flux ratio $\psi = 0.8$: $\square$, $\hat{F}_1 = 125$, $\chi_0 = 1.0$; $\diamond$, $\hat{F}_1 = 150$, $\chi_0 = 5.0$.

plume separation. The results are also scaled in terms of F_1 rather than the sum of the two buoyancy fluxes. Results for four different values of ψ are shown in figures 16–19.

The volume flux in a plume is given by

$$Q = \left(\frac{5F}{4\alpha}\right)^{1/3}\left(\frac{6\alpha z}{5}\right)^{5/3}. \tag{4.6}$$

For $\alpha = 0.09$ this leads to the following expressions for the flow rate above and below the point of coalescence:

$$z_{below} = 2.28\left(1 + \psi^{1/3}\right)^{-1/3} Q^{3/5} F_1^{-1/5}, \tag{4.7}$$

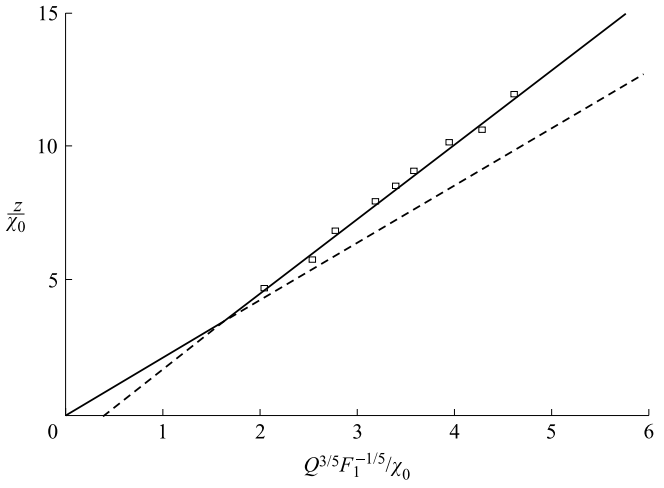

FIGURE 18. Flow rate measurements for two merging plumes of buoyancy flux ratio $\psi = 0.45$: $\hat{F}_1 = 131$, $\chi_0 = 1.0$.

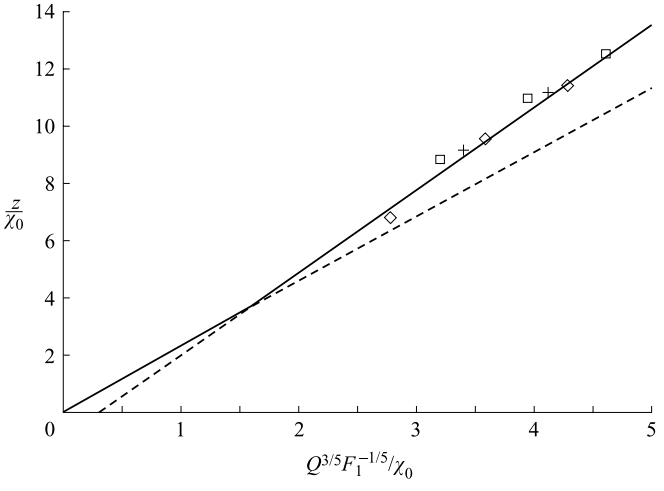

FIGURE 19. Flow rate measurements for two merging plumes of buoyancy flux ratio $\psi = 0.23$: $\hat{F}_1 = 129$, $\chi_0 = 1.0$, with different symbols representing different experimental runs.

and

$$z_{above} = 3.013(1+\psi)^{-1/5} Q^{3/5} F_1^{-1/5} + z_v. \tag{4.8}$$

where z_v is the asymptotic virtual origin for the merged plume as shown in figure 9. In the results presented below, the thick line is given by $\max(z_{below}, z_{above})$, and the thin line is given by $\min(z_{below}, z_{above})$. The data points should, therefore, follow the thick line.

The results for merging equal plumes are shown in figure 16. The theoretical prediction clearly provides a good fit for the experimental data, justifying its use. Further experimental results are shown in figures 17 to 19. Again they all show good agreement with the theoretical prediction for the flow rate and virtual origin of the combined plume.

5. Conclusions

This paper has examined the coalescence of two axisymmetric plumes rising from two sources separated horizontally. The point of coalescence of two co-flowing plumes is defined as the point at which the mean horizontal buoyancy profile of the combined flow has a single maximum. Assuming that the plumes are only passively advected by the entrainment field of each other, a theoretical prediction of the merging height was made (figure 6). Buoyancy profiles measured using a dye attenuation technique (figure 11) and a light-induced fluorescence (figure 12) showed that the mean buoyancy profiles behaved in a similar manner to that predicted. The prediction of the merging height ($\lambda_m = 4.8$ for equal plumes) was tested experimentally and found to over-predict λ_m slightly ($\lambda_m = 4.1$ for equal plumes, see figure 15 for unequal plume results). Various reasons for this discrepancy were suggested, particularly the sensitivity of the merging height to the entrainment coefficient. However, the model predicts the qualitative behaviour of the merging height as a function of the buoyancy flux ratio ψ for unequal plumes, that is the merging height decreases only slightly with ψ for $\psi > 0.25$. The model also accounts for over 80% of the reduction in merging height that results from the approach of the plumes as a result of their mutual entrainment.

Once a point of coalescence was established a calculation was made for the flow in the far field after the plumes had merged. This calculation resulted in a prediction of the virtual origin of the resulting single plume (figure 9) in terms of the buoyancy flux ratio ψ and the horizontal source separation. For equal plumes the virtual origin of the merged plume is found to be a distance below the sources of 1.4 times the source separation. Again this was tested against experimental data (figures 16 to 19), showing very good agreement with theory. This agreement in the prediction of the plume flow rate justifies the selected definition of the merging height, as the transition from two-plume to single-plume behaviour is observed to occur at this height. Measurements of the volume flux show that the two-plume to single-plume transition occurs over a vertical distance of the order of the source separation.

Although the model presented shows good qualitative and quantitative agreement with observations and experiment, it has significant limitations that require further work. The plumes have the same source height, although many examples of vertical as well as radial separation of plume sources exist. For example, two electronic components at different heights on an electronic circuit board will produce plumes with different source heights. A method for adapting this model to account for vertical separation is required.

N. B. K. would like to thank the British Council and the Association of Commonwealth Universities for their financial support for this research, and S. B. Dalziel for his assistance with the experimental part of this paper.

REFERENCES

Baines, W. D. 1983 A technique for the measurement of volume flux in a plume. *J. Fluid Mech.* **132**, 247–256.

Baines, W. D. & Turner, J. S. 1969 Turbulent buoyant convection from a source in a confined region. *J. Fluid Mech.* **37**, 51–80.

Batchelor, G. K. 1954 Heat convection and buoyancy effects in fluids. *Q. J. R. Met. Soc.* **80**, 339–358.

Bjorn, E. & Nielsen, P. V. 1995 Merging thermal plumes in the internal environment. *Proc. Healthy Buildings 95* (ed. M. Maroni).

Brahimi, M. & Doan-Kim-Son 1985 Interaction between two turbulent plumes in close proximity. *Mech. Res. Commun.* **12**, 149–155.

Cenedese, C. & Dalziel, S. B. 1998 Concentration and depth field determined by the light transmitted through a dyed solution. *Proc. 8th Intl Symp. Flow Visualization.*

Chen, C. J. & Rodi, W. 1980 *Vertical Turbulent Buoyant Jets.* Pergamon.

Ching, C. Y., Fernando, H. J. S., Mofor, L. A. & Davies, P. A. 1996 Interaction between multiple line plumes: a model study with application to leads. *J. Phys. Oceanogr* **26**, 525–540.

Dalziel, S. B., Linden, P. F. & Youngs, D. L. 1997 Self-similarity and internal structure of turbulence induced by Rayleigh-Taylor instability. *Proc. 6th Intl Workshop on the Physics of Turbulent Mixing* (ed. Young, Glimm & Boston), pp. 321–330. World Scientific.

Davidson, M. J., Papps, D. A. & Wood, I. R. 1994 The behaviour of merging buoyant jets. In *Recent Research Advances in the Fluid Mechanics of Turbulent Jets and Plumes* (ed. P. A. Davies & M. J. Valente Neves), pp. 465–478. Dordrecht.

Gaskin, S. J., Papps, D. A. & Wood, I. R. 1995 The axisymmetric equations for a buoyant jet in a cross flow. *Twelfth Australasian Fluid Mechanics Conference* (ed. R. W. Bilger), pp. 347–350.

George, W. K., Alpert, R. L. & Tamanini, F. 1977 Turbulence measurements in an axisymmetric buoyant plume. *Intl J. Heat Mass Transfer* **20**, 1145–1154.

Hunt, G. R. & Kaye, N. G. 2001 Virtual origin correction for lazy turbulent plumes. *J. Fluid Mech.* **435**, 377–396.

Hunt, G. R. & Linden, P. F. 2001 Steady-state flows in an enclosure ventilated by buoyancy forces assisted by wind. *J. Fluid Mech.* **426**, 355–386.

Linden, P. F. 1999 The fluid mechanics of natural ventilation. *Annu. Rev. Fluid Mech.* **31**, 201–238.

Morton, B. R. & Middleton, J. 1993 Scale diagrams for forced plumes. *J. Fluid Mech.* **58**, 165–176.

Morton, B. R., Taylor, G. I. & Turner, J. S. 1956 Turbulent gravitational convection from maintained and instantaneous sources. *Proc. R. Soc. Lond.* **234**, 1–23.

Moses, E., Zocchi, A. & Libchaber, A. 1993 An experimental study of laminar plumes. *J. Fluid Mech.* **251**, 581–601.

Nakagoma, H. & Hirata, M. 1977 The structure of turbulent diffusion in an axisymmetric turbulent plume. *Proc. 1976 ICHMT Seminar on Turbulent Buoyant Convection*, pp. 361–372.

Papanicolaou, P. N. & List, E. J. 1988 Investigations of round vertical turbulent buoyant jets. *J. Fluid Mech.* **195**, 341–391.

Pera, L. & Gebhart, B. 1975 Laminar plume interactions. *J. Fluid Mech.* **65**, 250–271.

Rouse, H., Baines, W. D. & Humphreys, H. W. 1953 Free convection over parallel sources of heat. *Proc. Phys. Soc.* B **66**, 393–399.

Rouse, H., Yih, C. S. & Humphreys, H. W. 1952 Gravitational convection from a boundary source. *Tellus* **4**, 201–210.

Shabbir, A. & George, W. K. 1994 Experiments in a round turbulent buoyant plume. *J. Fluid Mech.* **275**, 1–32.

Tritton, D. J. 1988 *Physical Fluid Dynamics.* Oxford Scientific Publications.

Turner, J. S. 1986 Turbulent entrainment: the development of the entrainment assumption, and its application to geophysical flows. *J. Fluid Mech.* **173**, 431–471.